Journal of Membrane Science 541 (2017) 300–311

Contents lists available at ScienceDirect

Journal of Membrane Science

journal homepage: www.elsevier.com/locate/memsci

Fouling-resistant ultrafiltration membranes prepared via co-deposition of dopamine/zwitterion composite coatings

Alon Y. Kirschner[a], Chia-Chih Chang[b], Sirirat Kasemset[a], Todd Emrick[b,*], Benny D. Freeman[a,*]

[a] University of Texas at Austin, Department of Chemical Engineering, Texas Materials Institute, Center for Energy and Environmental Resources, and Environmental and Water Resources Engineering, 10100 Burnet Road, Building 133, Austin, TX 78758, USA

[b] University of Massachusetts at Amherst, Polymer Science and Engineering Department, 120 Governors Drive, Amherst, MA 01003, USA

ARTICLE INFO

Keywords:
Surface modification
Polydopamine
Polymer zwitterions
Ultrafiltration
Threshold flux

ABSTRACT

Poly(2-methacryloyloxyethyl phosphorylcholine) (PMPC), a polymer zwitterion, is known to reduce biofouling and impart low friction characteristics to materials surfaces. Using a one-step solution coating process, we report the incorporation of PMPC into polydopamine (PD) coatings on ultrafiltration (UF) membranes for oil-water separations. Polysulfone UF membranes were surface-modified with either pure PD or a mixture of PD and PMPC (PD-PMPC). Unmodified and surface-modified membranes were characterized with respect to pure water permeance, contact angle, coating thickness, threshold flux and molecular weight cutoff (MWCO). Both types of modified membranes showed a significant decrease in contact angle compared to unmodified membranes, indicating an increase in hydrophilicity. PD-PMPC-modified membranes had a slightly lower underwater contact angle than PD-modified membranes, as well as a higher threshold flux. Constant flux crossflow fouling experiments were conducted on unmodified, PD-modified, and PD-PMPC-modified membranes using a soybean oil emulsion as a model foulant at fluxes near and below the measured threshold flux. The fouling profiles of membranes with similar pure water permeance values were compared to assess the effect of different coating materials and coating conditions on fouling. PD-PMPC-modified membranes exhibited the greatest fouling resistance. Zeta potential measurements showed only small differences in surface charge between the membranes. MWCO experiments showed no difference in nominal pore size or pore size distribution for the modified membranes, indicating that the difference in fouling performance is likely due to the strongly hydrophilic surface properties contributed by PMPC. PD-PMPC-modified membranes exhibited stable, low transmembrane pressure operation at fluxes where PD-modified and unmodified membranes suffered from rapid fouling and an unstable transmembrane pressure profile.

1. Introduction

The rapid increase in the world's population has raised awareness of the issue of access to clean water, and inspired research on membrane-based separations as an efficient, low-cost method of water treatment [1]. The so-called water-energy-food nexus [2,3] describes the interrelationship of clean water, energy production, and agriculture. For example, in hydraulic fracturing, drilling a single well requires 3–6 million gallons of water [4,5], of which ~30% returns to the surface as flowback water contaminated with salts, oils, heavy metals, and surfactants [6]. Currently, one of the most economical methods for disposing of contaminated water is deep well injection [5]. Environmental problems associated with this method include wasting water, pollution associated with transportation to approved injection sites [7], and a reported link between wastewater injection and earthquakes near disposal wells [8–10]. On-site testing has shown that treated flowback water can be reused for drilling additional wells with no danger to the integrity or productivity of the well [11].

In terms of treatment methodologies, membrane separation advantages include their small footprint, cost effectiveness, and ease of use relative to conventional technologies [12,13], making them prime candidates for treatment of hydraulic fracturing wastewater. However, membrane fouling remains a challenge, especially for highly concentrated feeds [14]. Fouling occurs as rejected solutes accumulate on the membrane surface, increasing mass transfer resistance, lowering water permeance and increasing the energy required to maintain constant throughput. Eventually, a cake layer of foulant forms on the membrane surface [15,16], requiring physical and/or chemical cleaning of the membrane or its replacement altogether [17], thereby increasing operating costs.

* Corresponding authors.
E-mail addresses: tsemrick@mail.pse.umass.edu (T. Emrick), freeman@che.utexas.edu (B.D. Freeman).

http://dx.doi.org/10.1016/j.memsci.2017.06.055
Received 29 March 2017; Received in revised form 20 June 2017; Accepted 22 June 2017
Available online 27 June 2017

In addition to feed pre-treatment [17], membranes can be tailored to resist fouling more effectively. Most commercial water filtration membranes are composed of hydrophobic polymers (*e.g.*, polysulfone and polyvinylidene fluoride), making them prone to fouling by hydrophobic foulants (*e.g.,* emulsified oil) *via* hydrophobic-hydrophobic interactions [12]. Greater surface hydrophilicity mitigates adsorption of foulants due to the presence of surface-bound water molecules, which obstruct foulant adhesion to the membrane surface [1,18]. Polymer membranes can be modified during their fabrication using additive blending, where surface modifying macromolecules (SMMs) are added to a polymer prior to membrane formation [19,20]. The SMMs preferentially migrate to the surface during the phase inversion process used in many ultrafiltration and microfiltration membrane preparations, effectively imparting their hydrophilic properties to the membrane surface [21]. For example, Ishihara fabricated cellulose acetate and polysulfone membranes by adding a phosphorylcholine-containing copolymer to the membrane casting solution, affording membranes with reduced protein fouling and enhanced hemocompatibility [22–24].

Membrane modification techniques [25] include plasma treatment [26,27], UV irradiation [28,29], chemical grafting of hydrophilic molecules to the membrane surface [30–32], and surface coating [33–35]. Messersmith discovered that polydopamine (PD), which has both the catechol and amine functionalities responsible for the remarkable underwater adhesion of mussels, effectively coats nearly any surface [36]. PD-modified ultrafiltration (UF), reverse osmosis (RO) and microfiltration (MF) membranes exhibited enhanced fouling resistance when challenged with an oily water emulsion, presumably due to increased hydrophilicity [37]. In a pilot study for flowback water treatment, PD-graft-PEG-coated UF modules were operated in parallel with unmodified modules, and the coated membranes showed improved fouling resistance against emulsified oil and other contaminants, as indicated by lower transmembrane pressure and an increased capacity for flux recovery after mild chemical cleaning [38].

In this work, the unique adhesive quality of PD was exploited in conjunction with the hydrophilic polymer zwitterion PMPC to prepare thin film coatings on membranes. Polymer zwitterions represent a special class of hydrophilic polymers featuring positive and negative charges on each repeat unit. Matsuyama modified RO membranes with PD and a 2-methacryloyloxyethyl phosphorylcholine (MPC) copolymer with 2-aminoethyl methacrylate by initially coating the membrane with PD, followed by application of the copolymer. The modified membrane exhibited improved resistance to biofouling during crossflow filtration of a bacterial suspension [39], a finding attributed to strong association of water with the polymer zwitterion [40,41]. We recently reported a one-step co-deposition method to produce a composite PD-PMPC coating that is much more hydrophilic than pristine PD coatings [42,43].

Reported here are commercially available flat-sheet polysulfone (PS) ultrafiltration membranes modified with PD-PMPC composite coatings using a one-step solution coating process. Pore size distributions of modified and unmodified membranes were compared using molecular weight cut-off (MWCO) experiments. The threshold flux of the membranes was evaluated by flux stepping experiments [44]. Constant flux crossflow fouling studies, using soybean oil-in-water emulsions, were conducted at fluxes below and near the threshold flux. Fouling performance of PD-PMPC-modified, PD-modified and unmodified membranes was compared for membranes having similar pure water permeance values, surface charge, and pore size distribution. We introduce a new methodology to separate the effects of surface modification *per se* (*e.g.,* changes in hydrophilicity and surface charge) on fouling from the effect of the surface modification on membrane pore size and pore size distribution. The effect of the presence of polymer zwitterions in the coating on fouling was analyzed. To our knowledge, such a study of fouling resistance and membrane properties has never been applied to surface modification study using polymeric zwitterions as the coating material.

2. Materials and methods

2.1. Materials

Flat-sheet polysulfone ultrafiltration membranes (PS20 and PS10) were purchased from Ultura Inc. (Oceanside, CA). MWCO values of PS20 and PS10 are 85 ± 1 kDa and 20 ± 2 kDa, respectively, determined by the MWCO method detailed below. Glass plates with dimensions of 20 cm × 28 cm were used to mount membranes for modification. Acrylic plastic frames of the same dimensions with a 15 cm × 23 cm hole in the center were purchased from Interstate Plastics (Austin, TX). Rubber gaskets with the same dimensions as the acrylic plastic frames were obtained from Advanced Gasket & Supply, Inc. (Fort Worth, TX). Further details are provided elsewhere [44–46]. Polysulfone (UDEL P-3500 LCD MB) was obtained from Solvay Specialty Polymers (Alpharetta, GA). Dopamine hydrochloride, Trizma hydrochloride (Tris-HCl), cyclopentanone, and poly(ethylene glycol) (PEG) molecular weight standards were purchased from Sigma Aldrich (St. Louis, MO). *n*-Decane was purchased from Alfa Aesar (Ward Hill, MA). Sodium hydroxide (NaOH) and ethanol were purchased from Fisher Scientific (Pittsburgh, PA). Soybean oil (Wesson) was obtained from a local super market. Xiameter OFX-0193 non-ionic, silicone-based surfactant was purchased from Dow Corning (Midland, MI). Silicon wafers (6″ diameter) were purchased from Nova Electronic Materials, LLC (Flower Mound, TX). All chemicals were used as received. Ultrapure water (18.2 MΩ-cm at 25 °C, < 5 ppb TOC) was obtained from a Millipore Milli-Q Advantage A10 water purification system (Billerica, MA). Tris buffer (15 mM) was prepared by dissolving 2.364 g of Tris-HCl in ultrapure water (1 L) and adjusting pH to 8.8 by adding sodium hydroxide. PMPC was synthesized as described previously (M_n 8.8 kDa, Polydispersity (PDI) = 1.1) [42,47].

2.2. Pretreatment and surface modification of membranes

PS20 UF membranes were pretreated using a previously developed pretreatment protocol [44,48,49]. Membranes were cut into sheets (20 cm × 28 cm), then slowly immersed in ethanol with the active side of the membrane facing down. To encourage complete wetting of the pores, the membranes remained in ethanol for 24 h. The membranes were rinsed thoroughly with ultrapure water then soaked in ultrapure water for 24 h to remove the ethanol. The membranes were stored in ultrapure water until use. For surface modification, as shown in Fig. 1, a membrane sheet was placed on a glass plate (active side up) and held in place by a rubber gasket and plastic frame sealed with large metal binder clips (1″ capacity).

Rocking platform shakers (Cat. No. 12620-906, VWR International LLC, Randnor, PA) operating at 30 tilts per minute and a tilt level of 4 provided a reproducible amount of oxygen needed for dopamine polymerization [36]. Freshly prepared solutions (100 mL per

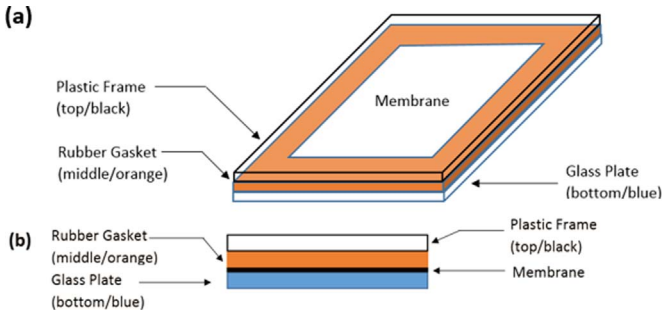

Fig. 1. (a) The front view and (b) the cross-sectional view of the membrane modification module employed in these studies.

Table 1
Membrane coating conditions and their influence on membrane permeance and contact angle I.

Membrane	[PMPC] (g/L)	[dopamine] (g/L)	Time (h)	Pure water permeance (LMH/bar)	Contact angle (°)
Unmodified PS20 (roll A)	–	–	–	1400 ± 120	88 ± 6
Unmodified PS20 (roll B)	–	–	–	900 ± 200 [49]	109 [49]
PD-1	–	2	2.5	950 ± 70	28 ± 5
PD-PMPC-1	2	2	0.5	920 ± 60	25 ± 3
PD-PMPC-2	2	0.8	0.5	920 ± 60	27 ± 2

*PS20 roll A was used for all surface modification studies.

membrane sheet) of dopamine or dopamine/PMPC mixtures were poured onto the membrane surface and remained in contact with the membrane for the prescribed time. At a desired deposition time, the membrane sheet was rinsed with ultrapure water and left in ultrapure water overnight to remove any weakly-bound material from the membrane surface. The ultrapure water was then replaced with fresh ultrapure water for storage until use.

To prepare a membrane sample according to modification condition PD-PMPC-1 in Table 1, two test tubes were filled with 50 mL of TRIS buffer each. 100 mg of dopamine hydrochloride and 100 mg of PMPC were then added to each test tube. The solution was mixed at a speed setting of 10 on a vortex mixer (Cat. No. 02-215-365, Fischer Scientific, Waltham, MA). As soon as the reagents were dissolved, the solutions from both tubes were poured onto the membrane surface and the rockers were activated at the setting detailed above. Membrane coating was performed at ambient temperature at a modification time (for this condition) of 30 min.

2.3. Pure water permeance

Pure water permeance was measured using a dead-end filtration system. Membranes were cut into circular samples using a punch die (4.3 cm diameter, Tecre, Fond du Lac, WI) and tested in UHP 43 stirred cells (Advantec MFS Inc., Dublin, CA). The cells were filled with ultrapure water, with the permeate tube flowing into a beaker placed on a mass balance (PR1203, Mettler Toledo). The cells were then pressurized with N_2 at 30 psig (2.1 bar), and the permeate mass was recorded using a LabVIEW® program (National Instruments). The pure water permeance was calculated using Eq. (1).

$$P = \frac{J}{TMP} \quad (1)$$

where J (liter/(m^2 h)) (LMH) is the steady state flux (calculated from the slope of mass change in the beaker over time divided by the membrane area), TMP (2.1 bar) is the transmembrane pressure, and P (LMH/bar) is the pure water permeance.

The membranes exhibited some variance in pure water permeance within a given roll. The direction in which the roll unwinds is the machine direction, and the direction perpendicular to that is the transverse direction. Most of the variance in membrane permeance was along the transverse direction. For example, membranes from a representative roll of as-received PS20 (Roll A) had a pure water permeance of 1400 ± 250 LMH/bar when samples spanning the transverse direction of the membrane were tested. However, at a given transverse position, the permeance exhibited much less variability in the machine direction. As an example, for the same roll of PS20 the standard deviation in the machine direction was ± 120 LMH/bar (cf., Table 1).

To minimize the effect of the variance in pure water permeance on the characterization of membrane fouling performance, the pure water permeance of each type of modified and unmodified membrane was first tested for 20 samples spanning the transverse direction. These results showed which region of the membrane had a pure water permeance closest to the average of the roll. Samples used in MWCO (cf., Section 2.4), flux-stepping (cf., Section 2.9), and constant flux crossflow fouling experiments (cf., Section 2.8) were harvested along the machine direction from those areas with the lowest deviation from the average pure water permeance. For MWCO experiments, samples taken from these specific areas were tested for pure water permeance prior to the MWCO experiment, and only those with values close to the average were used. For the crossflow system experiments, three samples taken from these specific areas in the membrane were placed in the sample cells of the crossflow system, and the feed flow rate and pressure were stabilized (using DI water) according to the method described by Miller *et al.* [50] Once the feed conditions stabilized, the permeate flow rate was set to 33 LMH. The pure water permeance reading experiences small fluctuations due to pressure changes, and this condition was selected for having relatively stable pure water permeance values. The pure water permeance for each sample was calculated as the average of the fluctuating values, and only samples with values close to the average pure water permeance were kept. Unsuitable samples were replaced by shutting down the system, replacing them, and repeating the process until all three samples had similar pure water permeance values. Consequently, the samples used for the crossflow and MWCO experiments have a lower standard deviation value (approximately ± 50 LMH/bar) than that measured for the 20 samples in the pure water permeance experiment, and the standard deviation values reported in Tables 1 and 2 represent membranes selected using the method described above (with the exception of unmodified PS20 Roll B, taken from Miller *et al.* [49]). For reference, Table S1 presents the standard deviation values of the membranes measured for 20 samples across the transverse direction.

2.4. Molecular weight cutoff (MWCO)

MWCO tests were run according to ASTM standard E1343 – 90 [51], except that the solute marker for rejection was poly(ethylene glycol) (PEG) instead of dextran. 0.1 wt% (1000 ppm) PEG solutions were made with an individual molecular weight precursor (4, 8, 10, 12, 20, 35, 100 and 200 kDa). Each solution was filtered individually through the membrane in increasing order of molecular weight using Amicon® 8200 (Millipore Corp.) dead-end filtration stirred cells. To reduce the effect of concentration polarization, stirring speed was set to 250 rpm, and permeate flow rate was kept low (0.17 ± 0.1 mL/min), which corresponds to a permeate flux of 0.0001 cm/s or 3.6 LMH [51].

Permeate collection began after circulating the PEG solution through the cells for 30 min to allow the system to reach steady state.

Table 2
Membrane coating conditions and their influence on membrane permeance and contact angle II.

Membrane	[PMPC] (g/L)	[dopamine] (g/L)	Time (h)	Pure water permeance (LMH/bar)	Contact angle (deg.)
Unmodified PS10	–	–	–	570 ± 30	36 ± 2
PD-2	–	4	1.5	630 ± 40	34 ± 9
PD-PMPC-3	2	0.8	4	680 ± 50	22 ± 0.3
PD-PMPC-4	2	5	0.5	590 ± 30	26 ± 4

*PS20 roll A was used for all surface modification studies.

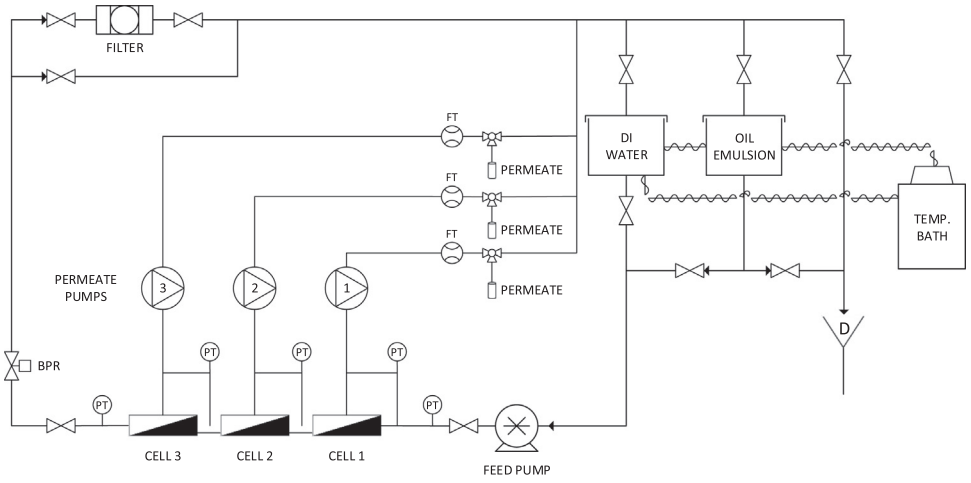

Fig. 2. Schematic of the crossflow fouling system employed in this work. (PT- pressure transducer, FT- flow transducer, BPR- back pressure regulator, D- drain).

Both membranes and cells were washed with ultrapure water between runs. The organic content of both feed and permeate solutions was analyzed using a total organic carbon analyzer (TOC-VCSH, Shimadzu Corp., Japan). A concentration polarization correction was applied to the results to calculate C_p/C_f [52,53], and the actual rejection was calculated using Eq. (2).

$$\%R = \left(1 - \frac{C_p}{C_f}\right) \cdot 100\% \tag{2}$$

where R is the percent rejection, and C_p/C_f is the ratio of permeate to feed concentrations, after the concentration polarization correction has been applied. An explanation of the concentration polarization correction is provided in the Supporting information.

Organic rejection curves were plotted as a function of PEG molecular weight. The MWCO of a specific membrane is the PEG molecular weight at which the organic rejection is 90% [51]. A nominal pore size was estimated by calculating Stokes radius of PEG at this molecular weight using Eq. (3) [54]:

$$a = 16.73 \cdot 10^{-3} M_w^{0.557} \tag{3}$$

where a is the Stokes radius of PEG (nm), and M_w is the PEG molecular weight (g/mol).

2.5. Contact angle (CA)

CA measurements were conducted with a goniometer (ramé-hart, model 200-F1) using the captive bubble method [55,56]. A thin strip of membrane (~3 mm wide) was mounted tightly in a sample holder with the active side down, and submerged in DI water. An *n*-decane droplet was deposited on the active side using a microliter syringe (Cole-Parmer, Vernon Hills, Illinois) equipped with a J-shaped needle. For each sample, six images of *n*-decane droplets were captured and analyzed by DROPimage Standard software. Each droplet was analyzed five times. The contact angle of each drop was taken as the average of these five measurements, and the reported standard deviation is calculated from the contact angle values of the six different droplets.

2.6. Chemical characterization of membrane surfaces

2.6.1. X-ray photoelectron spectra (XPS)

XPS were acquired using a Physical Electronics Quantum 2000 Microprobe instrument with a monochromatic Al 50-W X-ray source under ultrahigh vacuum and a 200 μm spot area. The take-off angle was fixed at 45°. High resolution scans were acquired to obtain chemical composition.

2.6.2. Fourier-transform infrared (FT-IR)

FT-IR spectra were recorded on a PerkinElmer Spectrum 100 spectrometer with an attenuated total reflectance (ATR) accessory.

2.7. Model foulant preparation

Fouling tests were conducted with a model oil/water emulsion with an organic concentration of 1500 ppm, similar to that used in previous studies [46,49]. The emulsion had a soybean oil-to-surfactant (OFX-0193) ratio of 9:1 (10.8 g oil: 1.2 g non-ionic surfactant) in 8 L of emulsion. Oil and surfactant were added to 1 L of ultrapure water in a commercial heavy duty blender (Waring Laboratory, Stamford, CT). After mixing at 20,000 rpm for 3 min, the emulsion was diluted with 7 L of DI water (making sure to wash all residue from the blender) and poured into the temperature controlled (*i.e.*, 25 °C) feed tank of the crossflow system.

2.8. Crossflow fouling experiments

Most industrial membrane separation processes are operated at constant flux [57,58]. Therefore, to examine the effect of surface modification on membrane fouling, a constant flux crossflow setup was used, as shown in Fig. 2 [50]. Three membrane samples were tested simultaneously. Peristaltic pumps (Cat. No. Drive: 7523-80 Head: 7519-20 Cartridge: 7519-75, Cole-Parmer, Vernon Hills, IL), controlled by feedback from permeate Coriolis flow meters (Cat. No. M13-ABD-11-0-S, Bronkhorst, Bethlehem, PA), maintained constant permeate flux through each sample cell. Permeate and feed streams were continuously recycled to the feed tank to maintain constant volume and concentration of the feed oil emulsion (with the only loss being the negligible amount of oil that fouled the membranes). Feed pressure was maintained at 30 psig (2.1 bar) using a back pressure regulator (Cat. No. EB1HF1, Equilibar, Fletcher, NC). A constant feed flow rate of 0.8 L/min was maintained using a gear pump (Cat. No. Drive: 75211-30 Head: 07003-04 Cole-Parmer, Vernon Hills, IL). While circulating DI water through the system, the flow was passed through a cartridge filter (Cat. No. Housing: 29820-11 Filter: 01508-93, Cole-Parmer, Vernon Hills, IL). While flowing the oil/water emulsion through the system, this filter was bypassed.

As a membrane fouls, its mass transfer resistance increases, so the TMP required to maintain constant flux increases. Using pressure transducers on each cell to monitor the change in TMP over time characterizes fouling resistance. Comparing unmodified and modified membranes with similar pure water permeance values helps isolate the contribution of the surface modification to the fouling behavior of the membranes [44]. Samples of the emulsion were collected at the beginning and end of the experiment, and permeate samples were

collected for each sample cell after 30 min of operation (to ensure permeate lines had been flushed with permeate). The organic content of both feed and permeate solutions was analyzed using a total organic carbon analyzer and rejection values were calculated using Eq. (2), without applying a concentration polarization correction.

2.9. Threshold flux measurement

The threshold flux was defined by Field as the flux below which the rate of membrane fouling is low, meaning the transmembrane pressure (TMP) rises slowly with time or volume of permeate produced [59]. Above the threshold flux, the rate of fouling increases sharply, and the TMP increases rapidly with time. In physical terms, above the threshold flux, foulant removal mechanisms operate more slowly than foulant deposition. For practical purposes, a higher threshold flux allows a membrane process to operate at higher throughput without experiencing unacceptably high fouling rates, resulting in a lower membrane area necessary to achieve a desired production capacity, and lower capital and maintenance costs. Higher threshold flux coincides with greater resistance to fouling.

Threshold flux measurements were performed using the flux stepping method described in detail elsewhere [44]. Generally, the flux was systematically increased from a low initial value in constant steps over set time periods (in this case 10 LMH every 20 min), while monitoring the change in TMP. The experiment was terminated when the TMP reached the feed pressure (30 psi). Several methods of analysis can be used to determine the value of the threshold flux from such experiments [44]. We used the method based on the departure from linearity of a plot of average TMP vs. flux (cf., Section 3.3) [60]. This experiment was conducted in the crossflow system described in Section 2.8.

3. Results and discussion

3.1. Modification conditions and their effects on membrane properties

One challenge in characterizing the effect of surface modification on membrane fouling is separating the effects associated with changes in surface characteristics (*e.g.,* changes in hydrophilicity, surface zeta potential. surface roughness) on fouling from the effect of changes in membrane pore size and pore size distribution [52]. Comparing performance of a membrane before and after surface modification neglects potential impacts of changes in pore size and pore size distribution caused by the surface modification [46,52]. To address this challenge, we used different rolls of PS membranes with different initial pure water permeance values (cf., Tables 1 and 2). Based on previous reports, membrane surface modification with PD led to reduced pore size and, in turn, decreased pure water permeance [52]. Samples of a PS20 UF membrane, with a high initial pure water permeance of 1400 ± 150 L m^{-2} h^{-1} bar^{-1} (LMH/bar), labeled “Roll A”, were modified under conditions that give pure water permeance values comparable to that of unmodified PS membranes from another roll (Roll B), which had a lower initial permeance. Table 1 lists membrane modification conditions resulting in a pure water permeance of ~900 LMH/bar, comparable to that of unmodified PS20 Roll B membranes. Table 2 lists conditions resulting in a pure water permeance of ~600 LMH/bar, comparable to the permeance of the unmodified PS10 roll. Comparing membranes with similar pure water permeance values facilitates isolation of the key factors contributing to enhanced fouling resistance [49].

PD and PD-PMPC composite coatings were deposited using the one-step solution coating process described in Section 2.2. Modified membranes turned brown, with the PD-modified membranes appearing darker than the PD-PMPC-modified membranes. Successful incorporation of PMPC in the PD-PMPC composite coatings was confirmed by FT-IR spectroscopy and XPS. The FT-IR spectra of PD-PMPC-modified membranes showed the methacrylate carbonyl signal at 1724 cm^{-1} and quaternary ammonium of the PC groups at 965 cm^{-1} (cf., Fig. S1a). XPS revealed the appearance of P_{2p} peaks at 132.4 eV and a quaternary ammonium N_{1s} signal at 401.6 eV, each characteristic of PMPC (cf., Fig. S1b and c). As expected, these IR and XPS signals were absent in the PD-modified membranes. High-resolution XPS revealed the presence of sulfur from the underlying PS membrane, suggesting that the deposited coatings on the membranes are very thin, since XPS experiments were performed at a sampling depth of ~4–5 nm (*i.e,* a take-off angle of 45°) [61–63].

Coating conditions, such as reagent concentration and deposition time, affect coating thickness, surface hydrophilicity, and overall membrane performance [52]. Values for these properties at different modification conditions are summarized in Tables 1 and 2.

The pure water permeance values of unmodified PS20 Roll A and Roll B differed significantly. The two rolls belonged to different lots. Roll A had a thickness of 193 ± 8 μm, and Roll B had a thickness of 209 ± 6 μm. Roll A was on average ~15 ± 6 μm thinner than Roll B, suggesting its skin layer was thinner than that of Roll B, which can explain at least some of this variability. The pure water permeance of the PS20 Roll A UF membrane decreased from 1400 ± 120 LMH/bar to 920 ± 60 LMH/bar after surface modification from a solution containing 0.8 g/L dopamine and 2.0 g/L PMPC for 0.5 h (PD-PMPC-2), and further decreased to 680 ± 50 LMH/bar after 4.0 h (PD-PMPC-3) as the coating thickened. PD-PMPC-modified membranes with a permeance of 920 ± 60 LMH/bar were also obtained after 0.5 h when the initial dopamine concentration was increased to 2.0 g/L and the PMPC concentration remained at 2.0 g/L (PD-PMPC-1). At a higher dopamine concentration of 5.0 g/L, and PMPC concentration of 2.0 g/L, the pure water permeance of the modified membrane decreased further to 590 ± 30 LMH/bar in 0.5 h (PD-PMPC-4). Membranes modified under conditions PD-PMPC-1 and PD-PMPC-2 had similar pure water permeance values despite PD-PMPC-2 having a lower dopamine concentration in the modifying solution (0.8 g/L compared to 2.0 g/L for PD-PMPC-1). Since these modifications were conducted at short times (30 min), the effect of a small change in dopamine concentration is not seen. Additionally, PD-PMPC coating thickness was approximated by ellipsometry by modifying spin-cast, nonporous PS films on silicon wafers using identical coating conditions employed for membrane modifications (for experimental details see Supporting information). Modified membranes with a pure water permeance of ~900 LMH/bar (*i.e.*, PD-PMPC-1, PD-PMPC-2) had thin coatings (~5–7 nm), while those with a pure water permeance of ~600 LMH/bar (*i.e.*, PD-PMPC-3, PD-PMPC-4) had coatings > 10 nm (see Supporting information Table S2) [49,52]. Table S2 shows that the thicknesses of PD-PMPC-1 and PD-PMPC-2 are very similar, measured as 7 ± 1 nm and 5 ± 2 nm, respectively. The increase of dopamine concentration to 5 g/L (PD-PMPC-4), caused a significant increase in the coating thickness to 16 ± 2 nm, and consequently a significant decrease in pure water permeance was observed. These results are in agreement with previous reports [49,52], suggesting the membrane permeance can be controlled by adjusting coating time and reagent concentrations. Furthermore, the presence of PMPC in the coating solution does not impair the ability to control the modified membrane's permeance.

Contact angle measurements assessed changes in surface hydrophilicity of modified membranes. The contact angle was measured by the underwater captive bubble method using *n*-decane as the probe liquid, so a lower contact angle value corresponds to greater hydrophilicity. Unmodified PS20 rolls A and B had contact angles of 88° and 109°, respectively. Despite this variability in contact angle, both PD and PD-PMPC-modified membranes were much more hydrophilic than the unmodified membranes, as shown in Table 1. PD-PMPC-modified membranes had slightly lower contact angles than PD-modified membranes, with PD-PMPC-modified membranes exhibiting contact angles ranging from 20° to 30°, and PD-modified membranes exhibiting contact angles of 28–34°. In our previous work, PD-PMPC-modified silicon wafers displayed much lower water contact angles in air (13° ± 0.5°)

than PD-modified silicon wafers (46° ± 2°), while their underwater chloroform contact angles differed only by ~5° [42]. Takahara and coworkers reported that hydrophilic surfaces may exhibit similar underwater hexadecane contact angle as the surface energy of modified surfaces approaches a threshold value, such that small differences in surface energy are difficult to discern regardless of the probe liquid employed [64].

Additionally, adhesion studies were performed with chloroform on PD and PD-PMPC modified silicon wafers tilted at a 2° angle. Chloroform droplets remained pinned to the PD-modified wafers but immediately rolled off of the PD-PMPC-modified wafers, again showing the improved hydrophilicity of the PD-PMPC modified surfaces despite the small difference in underwater contact angles [42]. The low contact angle of 36° observed for the unmodified PS10 membrane is presumably due to the presence of hydrophilic additives employed during membrane fabrication.

The effect of PMPC coatings on membrane surface charge was investigated using zeta potential measurements. At the pH of the oil/water emulsion used (~5.6), unmodified Roll B, PD-modified (PD-1) and PD-PMPC-modified (PD-PMPC-1) membranes had zeta potential values of −14.7 ± 1.5 mV, −16.8 ± 1.5 mV and −19.6 ± 1.5 mV, respectively (cf., Fig. S2), which is a rather small difference in zeta potential [65–67]. While surface charge can influence fouling [68], we speculate that the large change in surface hydrophilicity among these samples is the primary basis for the improved fouling resistance of PD-PMPC-modified membranes [42,46].

3.2. Molecular weight cutoff

Molecular weight cutoff (MWCO) experiments were conducted for both modified and unmodified membranes to evaluate the effect of surface modification on the nominal membrane pore size, pore size distribution, and MWCO, with results presented in Fig. 3 (plots without the concentration polarization correction are presented in Fig. S3). In Fig. 3a, the membranes with pure water permeance values ~900 LMH/bar are compared, and the rejection curve for unmodified PS-20 Roll A is given for reference. Both unmodified rolls have a similar MWCO (~85 kDa), but Roll B has lower pure water permeance, as mentioned in Section 3.1. Relative to unmodified PS20 Roll B, there is a decrease in the MWCO for both PD and PD-PMPC-modified samples. The MWCO values for the modified membranes are similar (PD-1 21 ± 2 kDa, PD-PMPC-1 25 ± 1 kDa) and lower than that of the unmodified PS20 rolls, confirming that surface modification decreases the nominal pore size. The slope of the MWCO curve is a qualitative indication of pore size distribution, with steeper curves suggesting narrower pore size distributions [69–72]. The steeper curves seen for the modified membranes indicate a narrower pore size distribution than in unmodified PS20. This may be due to blocking of small pores and/or narrowing of larger pores [52].

The reduced pore size may reduce internal fouling by allowing fewer oil droplets to penetrate into the membrane. However, this may also accelerate pore blockage and thus increase rates of external fouling. For membranes with pure water permeance values ~600 LMH/bar, the rejection curves for the unmodified PS10, the PD-2 and the PD-PMPC-4 membranes are nearly identical, with MWCO values of 20 ± 2 kDa, 16 ± 1 kDa and 17 ± 1 kDa respectively, supporting the hypothesis that the observed improvement in fouling resistance of the PD-PMPC-modified membranes (to be presented later) stems mainly from the increase in hydrophilicity afforded by the incorporation of PMPC into the coating, and not primarily from a difference in pore size. The PD-modified and PD-PMPC-modified samples with ~900 LMH/bar permeance exhibited comparable permeance and nominal pore radius on the same base polysulfone material. All three samples with ~600 LMH/bar permeance also had comparable permeance and nominal pore radius to each other. However, the PD-PMPC-modified membranes performed remarkably better in fouling experiments at higher flux, as will be discussed in Section 3.4.

3.3. Threshold flux

The fouling resistance of modified membranes was evaluated using constant flux crossflow experiments. First, the threshold flux was estimated using the flux stepping method [73,74], as shown in Fig. 4a. The analysis method to determine the threshold flux is shown in Fig. 4b. Threshold flux was estimated by monitoring the change in average TMP, which is calculated by first removing data corresponding to the first 2 min of each step (*i.e.*, the transition period between steps, before the TMP stabilizes), and then taking the arithmetic mean of the remaining TMP measurements during that step [44,73]. To determine the value of the threshold flux, a line was drawn through the points which exhibit a linear trend with an $R^2 \geq 0.99$, as shown in Fig. 4b [46]. At the point where the linear increase in flux with TMP ends, a second line is drawn through the next two points, and the threshold flux is defined as the flux at the intersection of the two lines. In the example in Fig. 4b, a linear trend was observed up to 90 LMH. Beyond that point, the slope of TMP_{avg} vs. flux increased rapidly, so the threshold flux was estimated to be 92.8 LMH. There was little variability among membranes with similar pure water permeance, as illustrated by the consistent threshold fluxes determined from each of the three flow cells (Fig. S4). The threshold fluxes of unmodified, PD-modified and PD-PMPC-modified membranes are reported in Tables 3 and 4. The threshold flux values were confirmed in constant flux experiments performed near the estimated threshold flux [73]. The uncertainty in the values was calculated by taking the standard deviation of the three sample cell measurements. Miller *et al.* showed that there is variance between the results of different methods for calculating the threshold flux, especially for modified membranes [44]. The method based on the departure from linearity of a plot of average TMP vs. flux was selected because it was typically the most accurate. However, threshold flux values estimated in this fashion should be confirmed with constant flux crossflow fouling experiments at fluxes below and above the estimated threshold flux [73].

Comparing membranes with a nominal pure water permeance of ~900 LMH/bar, PD-PMPC-1 and PD-PMPC-2 had nearly identical threshold fluxes of 92.8 ± 0.3 and 92.5 ± 0.7 LMH, respectively, higher than that of membrane PD-1 (75.7 ± 4.2 LMH). All three membranes had significantly higher threshold fluxes than that of unmodified PS20 Roll B (68 LMH), but with comparable pure water permeance. Comparing membranes with a nominal pure water permeance value of ~600 LMH/bar, the PD-modified membrane (PD-2) gave a lower threshold flux, 52.2 ± 0.5 LMH, than that of the unmodified PS10, 60.8 ± 1.3 LMH, while the PD-PMPC-modified membranes (PD-PMPC-3 and PD-PMPC-4) had much higher threshold fluxes than both PD-modified and unmodified membranes. PD-PMPC-4 was surface-modified under similar conditions as PD-PMPC-1, changing only the initial dopamine concentration from 2 to 5 g/L. PD-PMPC-3 was modified under similar conditions as PD-PMPC-2, changing only the deposition time from 0.5 h to 4 h. PD-PMPC-3 and -4 exhibited similar threshold flux values.

Extensive surface modification (*e.g.*, higher concentrations of modifying agents) results in a decrease in threshold flux. These results agree with previous investigations by Kasemset, et al., where higher concentrations and longer deposition times were observed to increase coating thickness and change membrane permeance, mean pore size and pore size distribution, resulting in reduced threshold flux values in some cases [52]. More aggressive coating conditions blocked some smaller pores and resulted in a narrowing of larger ones [52]. Since the membranes are tested at constant flux, open pores remaining after surface modification must transport more permeate (if the modification blocks smaller pores, for example) and as such are exposed to a higher foulant concentration resulting in lower threshold flux [46].

Fouling behavior was analyzed by plotting TMP against the ratio of

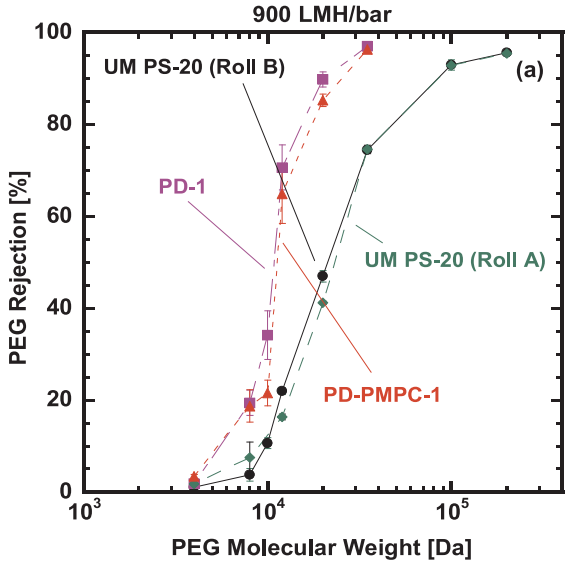

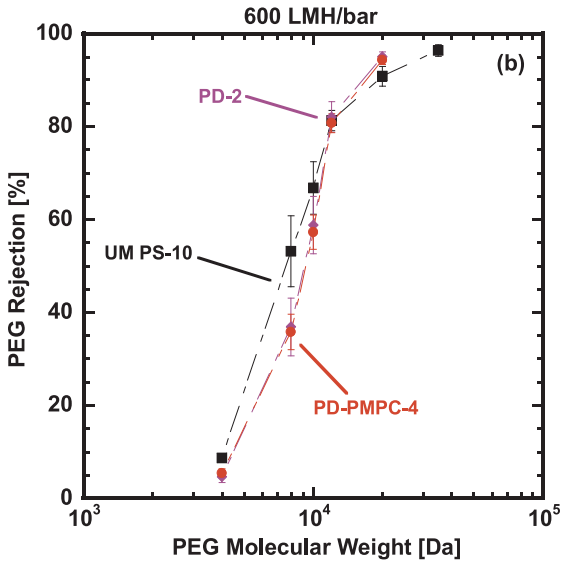

Sample name	MWCO [kDa]	a [nm]
Unmodified PS20 (Roll A)	85±5	9.3±0.3
Unmodified PS20 (Roll B)	85±1	9.3±0.1
PD-1	21±2	4.3±0.2
PD-PMPC-1	25±1	4.7±0.1

Sample name	MWCO [kDa]	a [nm]
Unmodified PS10	20±2	4.1±0.3
PD-2	16±1	3.7±0.2
PD-PMPC-4	17±1	3.8±0.1

Fig. 3. MWCO profiles of samples with permeance values of: **(a)** ~900 LMH/bar and **(b)** ~600 LMH/bar, and tables with the corresponding MWCO values. Actual rejection values were based on TOC of permeate collected after 30 min and feed collected at the start and end of each experiment, after applying a concentration polarization correction as described in the literature [52,53]. The MWCO for a sample is defined as the PEG molecular weight at which the rejection is 90% [51].

permeate volume divided by filtration area (V/A), which is a measure of how much feed solution has been processed by the membrane. Because the membrane is operated at constant flux, V/A is proportional to the run time of a fouling experiment [48]. Threshold flux confirmation was accomplished by running constant flux experiments in three flux regimes: (I) significantly below the threshold flux; (II) near the threshold flux; and (III) significantly above the threshold flux. Fig. 5 shows results for constant flux experiments on PD-PMPC-1, which has a threshold flux of 92.8 ± 0.3 LMH (cf., Table 3), run at 55, 85 and 115 LMH and PD-PMPC-4, which has a threshold flux of 76.2 ± 4.5 LMH, at 55, 75 and 115 LMH. These plots clearly illustrate the difference in operation below and above the threshold flux. For all fouling experiments, similar trends were observed, with small differences in TMP values, thus the data presented represent the sample with intermediate TMP values among the three cells.

Below the threshold flux, after an initial rise in TMP, the process reaches a stable point and can continue over a long timeframe with little-to-no additional fouling [59]. Above the threshold flux, the TMP rapidly increases until reaching the feed pressure. At this point, the experiment is terminated, since the permeate pressure has decreased to atmospheric pressure, and continuing the experiment may cause air bubbles to form in the permeate line, disrupting the flow control loop [49]. This rapid rise in TMP indicates strong fouling, where foulants are deposited onto the membrane surface faster than they are removed [75]. Membrane-based separation processes are typically operated well below the threshold flux to maintain stable operation at constant TMP.

As seen in Tables 3 and 4, PD-PMPC-modified membranes are capable of operation at significantly higher threshold flux than unmodified membranes with similar pure water permeance values. The increase in threshold flux suggested that the PD-PMPC-modified membranes can be operated sustainably at higher fluxes than either the unmodified membranes or the PD-modified membranes. Consequently, a comparison of fouling behavior for unmodified, PD-modified and PD-PMPC-modified membranes was conducted using constant flux crossflow fouling experiments on samples with pure water permeance values of nominally 900 LMH/bar and samples with pure water permeance values of nominally 600 LMH/bar, both at low flux and at a flux near the measured threshold flux of the PD-PMPC membrane.

3.4. Constant flux crossflow fouling

The unmodified, PD-modified and PD-PMPC-modified PS20

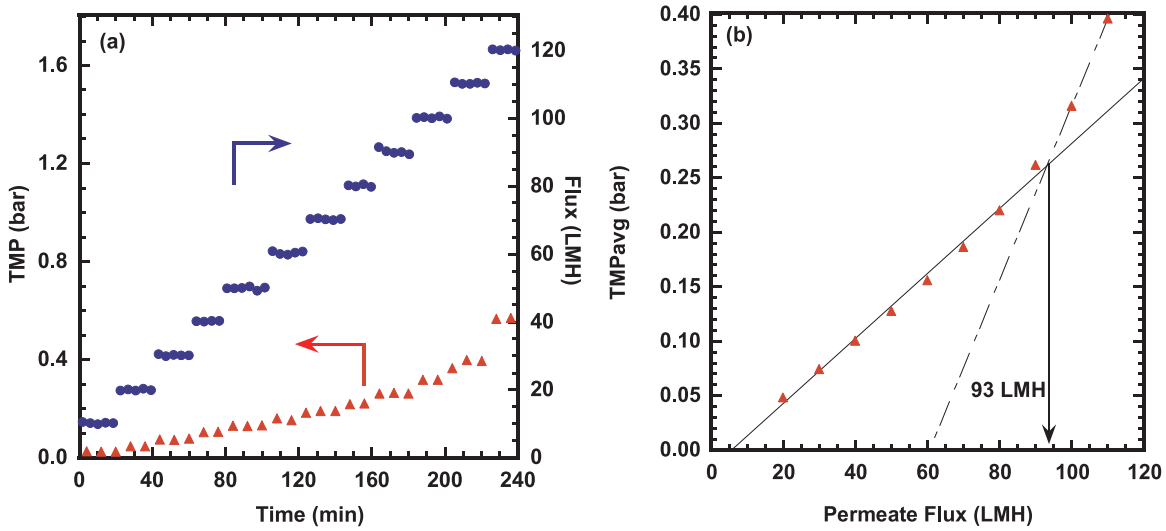

Fig. 4. Threshold flux determination of modified UF membranes (PD-PMPC-1) challenged with 1500 ppm soybean oil emulsion field. (a) Flux stepping experiment with stepwise flux increase by 10 LMH every 20 min. Initial Flux: 10 LMH. Feed pressure: 2.1 barg, crossflow velocity: 0.18 m/s (Reynolds number (Re) = 1000); (b) Threshold flux determination. The average TMP of each flux step is plotted against permeate flux. The threshold flux value is shown by the arrow pointing to the permeate flux axis.

Table 3
Threshold fluxes of unmodified, PD-modified, and PD-PMPC-modified PS UF membranes with permeance ~900 LMH/bar.

Membrane	Threshold flux (LMH)
Unmodified PS20 (Roll B)	68 [49]
PD-1	75.7 ± 4.2
PD-PMPC-1	92.8 ± 0.3
PD-PMPC-2	92.5 ± 0.7

Table 4
Threshold fluxes of unmodified, PD-modified, and PD-PMPC-modified PS UF membranes with permeance ~600 LMH/bar.

Membrane	Threshold flux (LMH)
Unmodified PS10	60.8 ± 1.3
PD-2	52.2 ± 0.5
PD-PMPC-3	77.3 ± 4.9
PD-PMPC-4	76.2 ± 4.5

membranes were subjected to constant flux crossflow fouling using a 1500 ppm soybean oil-in-water emulsion while monitoring the TMP. As the membrane fouls and some pores become less accessible or blocked by foulants, the local flux through the remaining open pores increases, and the rate of fouling can rise rapidly.

Fig. 6 compares constant flux results for unmodified, PD-modified and PD-PMPC-modified membranes at 55 and 85 LMH. As shown in Fig. 6a, at 55 LMH, the TMP of all three membranes reached a plateau for V/A > 1.4 cm, exhibiting similar trends of an initial rise in TMP followed by stabilization. This result is expected, since below the threshold flux, fouling is slow enough that the samples maintain relatively stable, long-term operation. Although PD-1 is more hydrophilic than unmodified PS20 Roll B, it exhibited a higher transmembrane pressure at 55 LMH. This flux is still well below the estimated threshold flux for both of these membranes, so neither membrane exhibits significant fouling. PD-1 has a lower nominal pore size than unmodified PS20 Roll B, which outweighs the effect of greater hydrophilicity under such low fouling conditions, resulting in a higher TMP. In Fig. 6b, at 85 LMH, there is a distinct difference between the fouling results for the

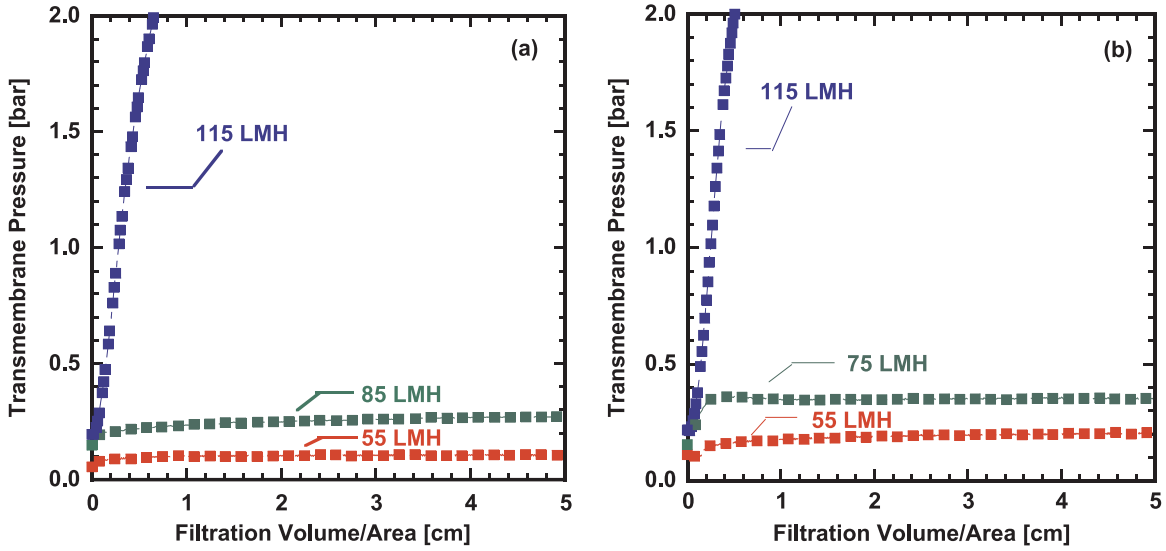

Fig. 5. The effect of permeate flux on fouling of PS20 UF membranes modified with: **(a)** PMPC 2 g/L and PD 2 g/L for 0.5 h (PD-PMPC-1) and **(b)** 2 g/L of PMPC and 5 g/L of PD for 0.5 h (PD-PMPC-4). Constant flux fouling experiments at 55, 75, 85 and 115 LMH were performed with a 1500 ppm soybean oil emulsion feed (3 samples per experimental set). The data presented is from the cell with intermediate TMP values. Feed pressure: 2.1 barg, crossflow velocity: 0.18 m/s (Re = 1000).

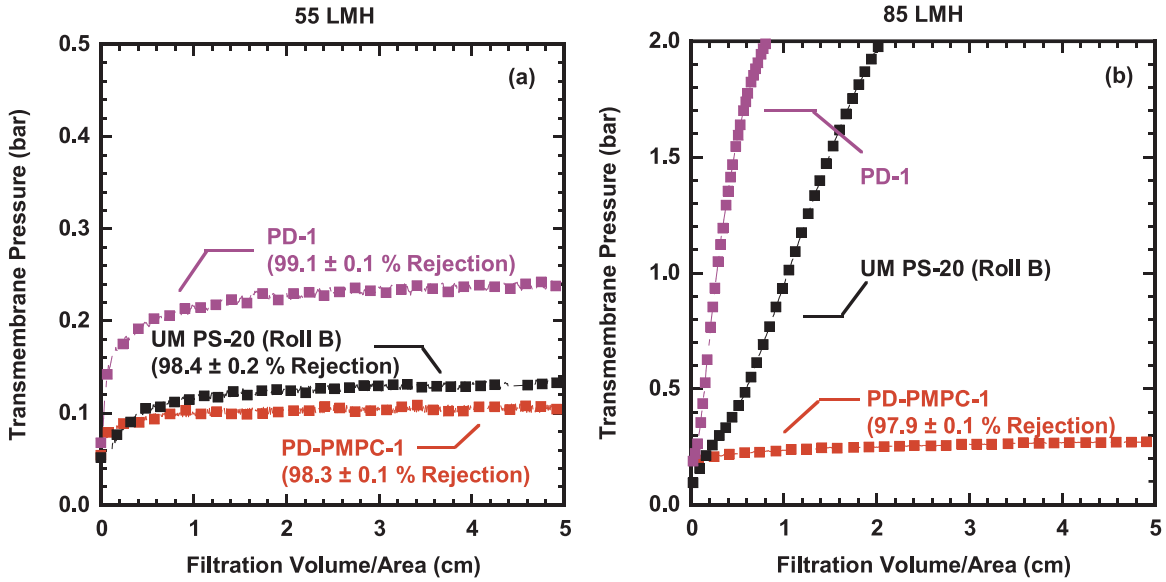

Fig. 6. Constant flux comparison of unmodified PS20 Roll B, PS20 modified with PD 2 g/L 2.5 h (PD-1), and PS20 modified with PMPC 2 g/L PD 2 g/L 0.5 h (PD-PMPC-1) at: **(a)** 55 LMH and **(b)** 85 LMH. Constant flux fouling experiments were run with a 1500 ppm soybean oil emulsion feed. Each experiment tested 3 samples, and the plot presented is of the cell with intermediate TMP values. Feed pressure: 2.1 barg, crossflow velocity: 0.18 m/s (Re = 1000).

PD-PMPC-modified sample and the unmodified and PD-modified samples. The PD-PMPC-modified sample reaches a stable TMP level of ~0.35 bar, higher than that at 55 LMH (~0.12 bar), but still presenting a stable fouling trend similar to that at the lower flux. In contrast, the unmodified and PD-modified membranes display a TMP profile that indicated rapid fouling, resembling that of Fig. 5 above the threshold flux. This result indicates a higher threshold flux and better fouling resistance for the PD-PMPC-modified membrane than for unmodified or PD-modified membranes with comparable pure water permeance. Between the PD-modified and unmodified membranes, TMP rapidly increased for the PD-modified membrane, and the experiment was stopped at V/A around 0.8 cm compared to about 2.1 cm for the unmodified membrane. At this flux both membranes are operating well above their estimated threshold flux and exhibit severe fouling. Again, the effect of lower nominal pore size for PD-1 outweighs its improved hydrophilicity. This finding matches previous reports that, in some cases, surface modification can actually exacerbate fouling [46]. For operation at a flux below the threshold flux of PD-1 and above that of the unmodified membrane *(e.g.,* 70 LMH), the PD-modified membrane will exhibit a lower TMP profile than the unmodified membrane.

In Fig. 7, a similar comparison was conducted for membranes with a nominal pure water permeance of 600 LMH/bar. These PD-PMPC-modified membranes maintained impressive fouling resistance even at this reduced permeance, despite their increased fouling potential as pore size decreases [46,52]. As before, at 55 LMH, below the measured threshold flux, all three samples exhibited excellent fouling resistance. The TMP profile of the unmodified PS10 membrane rose faster than that of the PD (PD-2) and PD-PMPC-modified (PD-PMPC-4) membranes, but it stabilized near the end of the experiment. As mentioned in Section 3.3, constant flux crossflow fouling experiments confirmed the estimated threshold flux determined by flux-stepping experiments. Although the threshold flux estimated for the PD-2 sample was 52.2 ± 0.5 LMH, the constant flux experiment showed a stable profile indicating operation below the threshold flux. In this case, the flux-stepping experiment appears to underestimate the threshold flux for this sample. Using an alternative method to estimate threshold flux, which tracks dTMP/dt at each step in the flux-stepping experiment, gives an estimated threshold flux of 71 ± 7 LMH (Fig. S5), which better describes the fouling behavior of the PD-2 membrane, and is consistent with previous studies [44,46]. At 75 LMH, above the estimated threshold flux of the unmodified PS10 and PD-modified PS20 membrane (PD-2), the PS10 membrane fouled rapidly, as shown by a rapid increase in TMP. The TMP of the PD-modified membrane (PD-2) also rose quickly until a V/A value of ~2 cm. However, in contrast to other membranes operating above the threshold flux, the TMP began stabilizing and approached a plateau at 1.9 bar at a V/A value of 3.4 cm. This is consistent with the observation that the threshold flux of PD-2 was underestimated in the flux-stepping analysis. TMP stabilization following a steep rise, such as that exhibited by the PD-modified membrane (PD-2) at 75 LMH, has been seen before in constant flux crossflow fouling with MF membranes [76,77]. In those cases, the membrane fouls slowly until enough pores are blocked for the threshold flux to decrease below the operating flux. At this point, a "TMP jump" occurs, where the membrane fouls rapidly and the TMP increases rapidly as a cake layer of foulant forms. Eventually, the cake grows to a point where the shear and drag forces are balanced, and the TMP profile reaches a plateau [76,77]. In our experiment, the PD-modified membrane (PD-2) is operating above its threshold flux from the outset of the experiment, resulting in the steep increase in TMP, followed by stabilization as the cake layer reaches steady state. The reason this stabilization is not observed for the other membranes operated above their threshold flux values is that those membranes are operating further above their threshold flux than PD-2, and the TMP surpasses 2.1 bar in the initial rapid fouling stage. Once the TMP reached the feed pressure, the experiment was terminated to avoid the introduction of air bubbles into the permeate line [50].

In contrast to the unmodified PS-10 and PD-modified (PD-2) membranes, the TMP profile of the PD-PMPC-modified membranes remained stable at 0.35 bar, with only a small increase in TMP during the early stage of the experiment (V/A < 0.2 cm), which is commonly observed in constant-flux fouling experiment due to concentration polarization and initial fouling [48,78,79].

In Figs. 6 and 7, oil rejection results are presented for experiments operated for at least 30 min, to allow for permeate sample collection. All membranes tested in this study had oil rejection values ~98%-99%. The diameter of the oil droplets in the fouling emulsion (~3.4 μm) was very large compared to the membrane pore size, so surface modification did not have a significant impact on the oil rejection.

Regarding the fouling resistance of the membranes, PD-PMPC-modified membranes significantly outperformed the unmodified and PD-modified membranes. For membranes with a pure water permeance of ~900 LMH/bar, PD-PMPC-modified samples had a slightly lower

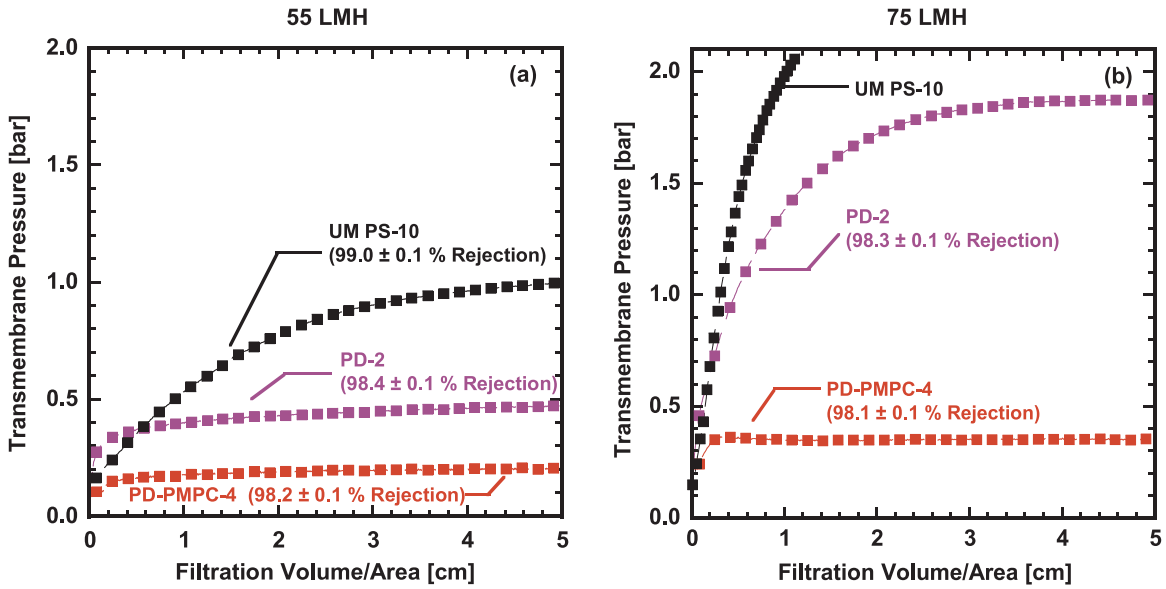

Fig. 7. Constant flux comparison of unmodified PS10, PS20 modified with PD 4 g/L 1.5 h (PD-2), and PS20 modified with PMPC 2 g/L PD 5 g/L 0.5 h (PD-PMPC-4) at: **(a)** 55 LMH and **(b)** 75 LMH. Constant flux fouling experiments were run with a 1500 ppm soybean oil emulsion feed. Each experiment tested 3 samples, and the plot presented is of the cell with the intermediate TMP values. Feed pressure: 2.1 barg, crossflow velocity: 0.18 m/s (Re = 1000).

TMP at 55 LMH compared to the unmodified and PD-modified membranes. At 85 LMH, the PD-PMPC-modified membranes exhibited stable, low TMP profiles, while the unmodified and PD-modified membranes experienced severe fouling and a sharp rise in TMP. For membranes with a pure water permeance of ~600 LMH/bar, PD-PMPC-modified samples had much lower TMP at 55 LMH compared to the unmodified and PD-modified membranes. At 75 LMH, the PD-PMPC-modified membranes exhibited stable, low TMP profiles compared to the unmodified and PD-modified membranes. PD-PMPC-1 afforded improvement in threshold flux of at least 25% compared to the threshold flux exhibited by unmodified PS20 Roll B, and PD-PMPC-2 gave a nearly 20% threshold flux improvement compared to PD-1. PD-PMPC membranes also exhibited low, stable TMP levels at all fluxes compared to the unmodified and PD-modified membranes. This finding is consistent with the hypothesis that the increased hydrophilicity due to the presence of the PC functional group in the surface coating reduces the hydrophobic attractive forces between the oil droplets and the membrane, weakening their ability to adhere to the surface, thereby increasing the viable stable operating flux. The simple co-deposition of polymer zwitterions and polydopamine on UF membranes opens new opportunities to exploit the adhesive characteristics of polydopamine and improve its fouling resistance with co-deposited polymer zwitterions. Such substantial improvements in fouling resistance, as observed in this study, hold promise for reducing the frequency of membrane cleaning, and overall operating costs, in a large scale, membrane-based water purification system.

4. Conclusions

We have demonstrated that a composite coating containing polydopamine and PMPC on UF membranes results in improved fouling resistance against oily water emulsions, particularly at elevated permeate rates. Polysulfone UF membranes were modified with PD-PMPC composite coatings. The presence of PMPC was verified by XPS and FTIR spectroscopy. Membranes were also modified with only PD, for comparison of fouling performance. Surface modifications were conducted on membrane samples from a membrane roll with high permeance (~1400 LMH/bar) and modification conditions were adjusted to enable proper comparisons to unmodified membranes with lower permeances of ~900 LMH/bar (PS20) and ~600 LMH/bar (PS10). The modified and unmodified membranes were characterized for pure water permeance, contact angle, and threshold flux. Additionally, the coating thicknesses were measured. Compared to unmodified samples, modified membranes displayed a significantly lower underwater contact angle with *n*-decane, indicating their greater surface hydrophilicity.

After determining the PD-PMPC threshold flux in flux-stepping experiments and verifying these results with constant flux fouling experiments, the unmodified, PD-modified and PD-PMPC-modified membranes were challenged with a soybean oil-in-water emulsion at fluxes below, and near, the threshold flux of the PD-PMPC-modified membranes. The PD-PMPC samples displayed a low TMP and stable operation at the experimental conditions considered, while the unmodified and PD-modified membranes exhibited rapid fouling when operated above their threshold flux. At a given flux, the lower TMP exhibited by the PD-PMPC-modified membranes relative to unmodified and PD-modified membranes is indicative of lower mass transfer resistance, confirming improved fouling resistance of the PD-PMPC-modified membranes. Using MWCO experiments, the effects of membrane coatings on surface properties was separated from the effect on pore size distribution. Zeta potential measurements showed only small differences in surface charge among the membrane samples studied. The increase in surface hydrophilicity, afforded by the presence of PMPC in the composite coating of the modified membrane, is therefore speculated to be the primary basis for the improved fouling resistance of PD-PMPC-modified membranes. Overall, the successful co-deposition of PD and PMPC on membrane surfaces opens opportunities for continued investigations and an expansion of the concept in which PD acts as a robust platform for the integration of non-fouling co-adsorbates.

Acknowledgements

The authors gratefully acknowledge financial support from the National Science Foundation CBET-1403670 and CBET-1403742, as well as partial support of this work by the Australian-American Fulbright Commission for the award to BDF of the U.S. Fulbright Distinguished Chair in Science, Technology and Innovation sponsored by the Commonwealth Scientific and Industrial Research Organization (CSIRO).

Appendix A. Supporting information

Supplementary data associated with this article can be found in the online version at http://dx.doi.org/10.1016/j.memsci.2017.06.055.

References

[1] G.M. Geise, H. Lee, D.J. Miller, B.D. Freeman, J.E. McGrath, D.R. Paul, Water purification by membranes: the role of polymer science, J. Polym. Sci.: Part B: Polym. Phys. 48 (2010) 1685–1718.

[2] M. Bazilian, H. Rogner, M. Howells, S. Hermann, D. Arent, D. Gielen, P. Steduto, A. Mueller, P. Komor, R.S.J. Tol, K.K. Yumkella, Considering the energy, water and food nexus: towards an integrated modelling approach, Energy Policy 39 (2011) 7896–7906.

[3] M. Bridges, K. Meehan, Overview of the water-energy nexus in the United States, 2014⟨http://www.ncsl.org/research/environment-and-natural-resources/overviewofthewaterenergynexusintheus.aspx⟩.

[4] L.P. Galusky, Fort Worth Basin/Barnett shale natural gas play: An assessment of present and projected fresh water use, 2007⟨http://www.shaledigest.com/documents/water/Barnett%20Shale%20Water%20Report%20Dr%20Pete%20Galusky%204-2007.pdf⟩.

[5] EPA hydraulic fracturing study technical workshop #4 water resources management, ⟨https://www.epa.gov/sites/production/files/documents/09_Mantell_-_Reuse_508.pdf⟩, 2011.

[6] S. Rassenfoss, From flowback to fracturing: water recycling grows in the Marcellus shale, J. Pet. Technol. 63 (2011) 48–51.

[7] R.F. Service, Desalination freshens up, Science 313 (2006) 1088–1090.

[8] E. Hand, Geoscience injection wells blamed in Oklahoma earthquakes, Science 345 (2014) 13–14.

[9] R.S. Bailey, Ground water contamination – fracking controversy continues, 2011⟨http://www.thelosangelespost.org/fracking-controversy-continues/⟩.

[10] K.M. Keranen, M. Weingarten, G.A. Abers, B.A. Bekins, S. Ge, Sharp increase in central Oklahoma seismicity since 2008 induced by massive wastewater injection, Science 345 (2014) 448–451.

[11] J. Papso, M. Blauch, D. Grottenthaler, Cabot gas well treated with 100% reused frac fluid, Superior Well Services, 2010.

[12] J. Mueller, Y. Cen, R.H. Davis, Crossflow microfiltration of oily water, J. Membr. Sci. 129 (1997) 221–235.

[13] R.W. Baker, Membrane Technology and Applications, 2nd ed, John Wiley & Sons Ltd, West Sussex, England, 2004.

[14] G. Belfort, R.H. Davis, A.L. Zydney, The behavior of suspensions and macromolecular solutions in crossflow microfiltration, J. Membr. Sci. 96 (1994) 1–58.

[15] R. Zhang, Y. Liu, M. He, Y. Su, X. Zhao, M. Elimelech, Z. Jiang, Antifouling membranes for sustainable water purification: strategies and mechanisms, Chem. Soc. Rev. (2016).

[16] A.D. Marshall, P.A. Munro, G. Tragardh, The effect of protein fouling in microfiltration and ultrafiltration on permeate flux, protein retention and selectivity - a literature review, Desalination 91 (1993) 65–108.

[17] W.X. Zhang, J.Q. Luo, L.H. Ding, M.Y. Jaffrin, A review on flux decline control strategies in pressure-driven membrane processes, Ind. Eng. Chem. Res. 54 (2015) 2843–2861.

[18] S. Mondal, S.R. Wickramasinghe, Produced water treatment by nanofiltration and reverse osmosis membranes, J. Membr. Sci. 322 (2008) 162–170.

[19] J.F. Hester, P. Banerjee, Y.Y. Won, A. Akthakul, M.H. Acar, A.M. Mayes, ATRP of amphiphilic graft copolymers based on PVDF and their use as membrane additives, Macromolecules 35 (2002) 7652–7661.

[20] D.B. Mosqueda-Jimenez, R.M. Narbaitz, T. Matsuura, Manufacturing conditions of surface-modified membranes: effects on ultrafiltration performance, Sep. Purif. Technol. 37 (2004) 51–67.

[21] D.E. Suk, T. Matsuura, H.B. Park, Y.M. Lee, Synthesis of a new type of surface modifying macromolecules (nSMM) and characterization and testing of nSMM blended membranes for membrane distillation, J. Membr. Sci. 277 (2006) 177–185.

[22] H. Ueda, J. Watanabe, T. Konno, M. Takai, A. Saito, K. Ishihara, Asymmetrically functional surface properties on biocompatible phospholipid polymer membrane for bioartificial kidney, J. Biomed. Mater. Res. Part A 77A (2006) 19–27.

[23] S.H. Ye, J. Watanabe, Y. Iwasaki, K. Ishihara, Antifouling blood purification membrane composed of cellulose acetate and phospholipid polymer, Biomaterials 24 (2003) 4143–4152.

[24] S.H. Ye, J. Watanabe, Y. Iwasaki, K. Ishihara, Novel cellulose acetate membrane blended with phospholipid polymer for hemocompatible filtration system, J. Membr. Sci. 210 (2002) 411–421.

[25] D. Miller, D. Dreyer, C. Bielawski, D. Paul, B. Freeman, Surface modification of water purification membranes: a review, Angew. Chem. Int. Ed., 2016, n/a-n/a.

[26] M. Ulbricht, G. Belfort, Surface modification of ultrafiltration membranes by low temperature plasma. I. Treatment of polyacrylonitrile, J. Appl. Polym. Sci. 56 (1995) 325–343.

[27] M. Ulbricht, G. Belfort, Surface modification of ultrafiltration membranes by low temperature plasma II. Graft polymerization onto polyacrylonitrile and polysulfone, J. Membr. Sci. 111 (1996) 193–215.

[28] N. Ehsani, S. Parkkinen, M. Nyström, Fractionation of natural and model egg-white protein solutions with modified and unmodified polysulfone UF membranes, J. Membr. Sci. 123 (1997) 105–119.

[29] M. Nyström, P. Järvinen, Modification of polysulfone ultrafiltration membranes with UV irradiation and hydrophilicity increasing agents, J. Membr. Sci. 60 (1991) 275–296.

[30] Y. Chang, C.Y. Ko, Y.J. Shih, D. Quemener, A. Deratani, T.C. Wei, D.M. Wang, J.Y. Lai, Surface grafting control of PEGylated poly(vinylidene fluoride) antifouling membrane via surface-initiated radical graft copolymerization, J. Membr. Sci. 345 (2009) 160–169.

[31] K. Ishihara, Y. Inoue, M. Kyomoto, Surface modification on poly(ether ether ketone) with phospholipid polymer via photoinduced self-initiated grafting, Macromol. Symp. 354 (2015) 230–236.

[32] M.Y. Zhou, H.W. Liu, J.E. Kilduff, R. Langer, D.G. Anderson, G. Belfort, High-throughput membrane surface modification to control NOM fouling, Environ. Sci. Technol. 43 (2009) 3865–3871.

[33] J.T. Arena, B. McCloskey, B.D. Freeman, J.R. McCutcheon, Surface modification of thin film composite membrane support layers with polydopamine: enabling use of reverse osmosis membranes in pressure retarded osmosis, J. Membr. Sci. 375 (2011) 55–62.

[34] S. Akhtar, C. Hawes, L. Dudley, I. Reed, P. Stratford, Coatings reduce the fouling of microfiltration membranes, J. Membr. Sci. 107 (1995) 209–218.

[35] D. Li, H. Wang, Recent developments in reverse osmosis desalination membranes, J. Mater. Chem. 20 (2010) 4551–4566.

[36] H. Lee, S.M. Dellatore, W.M. Miller, P.B. Messersmith, Mussel-inspired surface chemistry for multifunctional coatings, Science 318 (2007) 426–430.

[37] B.D. McCloskey, H.B. Park, H. Ju, B.W. Rowe, D.J. Miller, B.J. Chun, K. Kin, B.D. Freeman, Influence of polydopamine deposition conditions on pure water flux and foulant adhesion resistance of reverse osmosis, ultrafiltration, and microfiltration membranes, Polymer 51 (2010) 3472–3485.

[38] D.J. Miller, X. Huang, H. Li, S. Kasemset, A. Lee, D. Agnihotri, T. Hayes, D.R. Paul, B.D. Freeman, Fouling-resistant membranes for the treatment of flowback water from hydraulic shale fracturing: a pilot study, J. Membr. Sci. 437 (2013) 265–275.

[39] H. Karkhanechi, R. Takagi, H. Matsuyama, Enhanced antibiofouling of RO membranes via polydopamine coating and polyzwitterion immobilization, Desalination 337 (2014) 23–30.

[40] H. Kitano, M. Imai, T. Mori, M. Gemmei-Ide, Y. Yokoyama, K. Ishihara, Structure of water in the vicinity of phospholipid analogue copolymers as studied by vibrational spectroscopy, Langmuir 19 (2003) 10260–10266.

[41] W. Feng, M.P. Nieh, S. Zhu, T.A. Harroun, J. Katsaras, J.L. Brash, Characterization of protein resistant, grafted methacrylate polymer layers bearing oligo(ethylene glycol) and phosphorylcholine side chains by neutron reflectometry, Biointerphases 2 (2007) 34–43.

[42] C.C. Chang, K.W. Kolewe, Y.Y. Li, I. Kosif, B.D. Freeman, K.R. Carter, J.D. Schiffman, T. Emrick, Underwater superoleophobic surfaces prepared from polymer zwitterion/dopamine composite coatings, Adv. Mater. Interfaces 3 (2016).

[43] K.W. Kolewe, K.M. Dobosz, K.A. Rieger, C.C. Chang, T. Emrick, J.D. Schiffman, Antifouling electrospun nanofiber mats functionalized with polymer zwitterions, ACS Appl. Mater. Interfaces 8 (2016) 27585–27593.

[44] D.J. Miller, S. Kasemset, L. Wang, D.R. Paul, B.D. Freeman, Constant flux crossflow filtration evaluation of surface-modified fouling-resistant membranes, J. Membr. Sci. 452 (2014) 171–183.

[45] W. Xie, G.M. Geise, B.D. Freeman, H.-S. Lee, G. Byun, J.E. McGrath, Polyamide interfacial composite membranes prepared from m-phenylene diamine, trimesoyl chloride, and a new disulfonated diamine, J. Membr. Sci. 403–404 (2012) 152–161.

[46] S. Kasemset, Z.W. He, D.J. Miller, B.D. Freeman, M.M. Sharma, Effect of polydopamine deposition conditions on polysulfone ultrafiltration membrane properties and threshold flux during oil/water emulsion filtration, Polymer 97 (2016) 247–257.

[47] N. Bhuchar, Z.C. Deng, K. Ishihara, R. Narain, Detailed study of the reversible addition-fragmentation chain transfer polymerization and co-polymerization of 2-methacryloyloxyethyl phosphorylcholine, Polym. Chem. 2 (2011) 632–639.

[48] D.J. Miller, S. Kasemset, D.R. Paul, B.D. Freeman, Comparison of membrane fouling at constant flux and constant transmembrane pressure conditions, J. Membr. Sci. 454 (2014) 505–515.

[49] D.J. Miller, D.R. Paul, B.D. Freeman, An improved method for surface modification of porous water purification membranes, Polymer 55 (2014) 1375–1383.

[50] D.J. Miller, D.R. Paul, B.D. Freeman, A crossflow filtration system for constant permeate flux membrane fouling characterization, Rev. Sci. Instrum. 84 (2013) 035003.

[51] Standard test method for molecular weight cutoff evaluation of flat sheet ultrafiltration membranes, in, ASTM International, West Conshohocken, PA, 2001.

[52] S. Kasemset, L. Wang, Z. He, D.J. Miller, A. Kirschner, B.D. Freeman, M.M. Sharma, Influence of polydopamine deposition conditions on hydraulic permeability, sieving coefficients, pore size and pore size distribution for a polysulfone ultrafiltration membrane, J. Membr. Sci. 522 (2017) 100–117.

[53] C. Causserand, S. Rouaix, A. Akbari, P. Aimar, Improvement of a method for the characterization of ultrafiltration membranes by measurements of tracers retention, J. Membr. Sci. 238 (2004) 177–190.

[54] S. Singh, K.C. Khulbe, T. Matsuura, P. Ramamurthy, Membrane characterization by solute transport and atomic force microscopy, J. Membr. Sci. 142 (1998) 111–127.

[55] E.M. VanWagner, A.C. Sagle, M.M. Sharma, Y.-H. La, B.D. Freeman, Surface modification of commercial polyamide desalination membranes using poly(ethylene glycol) diglycidyl ether to enhance membrane fouling resistance, J. Membr. Sci. 367 (2011) 273–287.

[56] S. Kasemset, A. Lee, D.J. Miller, B.D. Freeman, M.M. Sharma, Effect of polydopamine deposition conditions on fouling resistance, physical properties, and permeation properties of reverse osmosis membranes in oil/water separation, J. Membr. Sci. 425–426 (2013) 208–216.

[57] R.W. Field, K.-V. Peinemann, S.P. Nunes (Eds.), Membrane Technology: Membranes for Water Treatment, John Wiley & Sons, Weinheim, Germany, 2010, pp. 1–24.

[58] B. Alspach, S. Adham, T. Cooke, P. Delphos, J. Garcia-Aleman, J. Jacangelo, A. Karimi, J. Pressman, J. Schaefer, S. Sethi, Microfiltration and ultrafiltration membranes for drinking water, J. Am. Water Works Assoc. 100 (2008) 84–97.
[59] R.W. Field, G.K. Pearce, Critical, sustainable and threshold fluxes for membrane filtration with water industry applications, Adv. Colloid Interface Sci. 164 (2011) 38–44.
[60] K.Y. Choi, B.A. Dempsey, Bench-scale evaluation of critical flux and TMP in low-pressure membrane filtration, J. Am. Water Works Assoc. 97 (2005) 134–143.
[61] T. Moro, Y. Takatori, M. Kyomoto, K. Ishihara, K. Saiga, K. Nakamura, H. Kawaguchi, Surface grafting of biocompatible phospholipid polymer MPC provides wear resistance of tibial polyethylene insert in artificial knee joints, Osteoarthr. Cartil. 18 (2010) 1174–1182.
[62] K. Ishihara, T. Tsuji, Y. Sakai, N. Nakabayashi, Synthesis of graft copolymers having phospholipid polar group by macromonomer method and their properties in water, J. Polym. Sci. Part A: Polym. Chem. 32 (1994) 859–867.
[63] Y. Liu, Y. Inoue, S. Sakata, S. Kakinoki, T. Yamaoka, K. Ishihara, Effects of molecular architecture of phospholipid polymers on surface modification of segmented polyurethanes, J. Biomater. Sci. Polym. Ed. 25 (2014) 474–486.
[64] M. Kobayashi, Y. Terayama, H. Yamaguchi, M. Terada, D. Murakami, K. Ishihara, A. Takahara, Wettability and antifouling behavior on the surfaces of superhydrophilic polymer brushes, Langmuir 28 (2012) 7212–7222.
[65] Z.W. He, S. Kasemset, A.Y. Kirschner, Y.H. Cheng, D.R. Paul, B.D. Freeman, The effects of salt concentration and foulant surface charge on hydrocarbon fouling of a poly(vinylidene fluoride) microfiltration membrane, Water Res. 117 (2017) 230–241.
[66] S. Muthu, A. Childress, J. Brant, Propagation-of-uncertainty from contact angle and streaming potential measurements to XDLVO model assessments of membrane–-colloid interactions, J. Colloid Interface Sci. 428 (2014) 191–198.
[67] A.E. Childress, M. Elimelech, Effect of solution chemistry on the surface charge of polymeric reverse osmosis and nanofiltration membranes, J. Membr. Sci. 119 (1996) 253–268.
[68] Z. He, D.J. Miller, S. Kasemset, L. Wang, D.R. Paul, B.D. Freeman, Fouling propensity of a poly(vinylidene fluoride) microfiltration membrane to several model oil/water emulsions, J. Membr. Sci. 514 (2016) 659–670.
[69] S. Mochizuki, A.L. Zydney, Theoretical analysis of pore size distribution effects on membrane transport, J. Membr. Sci. 82 (1993) 211–227.
[70] A.S. Michaels, Analysis and prediction of sieving curves for ultrafiltration membranes: a universal correlation? Sep. Sci. Technol. 15 (1980) 1305–1322.
[71] L. Zeman, M. Wales, Polymer solute rejection by ultrafiltration membranes, in: A.F. Turbak (Ed.), ACS Symposium Series 154 (Synthetic Membranes: Volume II Hyper- and Ultrafiltration Uses), American Chemical Society, Washington, DC, 1981, pp. 411–434.
[72] P. Aimar, M. Meireles, V. Sanchez, A contribution to the translation of retention curves into pore size distributions for sieving membranes, J. Membr. Sci. 54 (1990) 321–338.
[73] S.P. Beier, G. Jonsson, Critical flux determination by flux-stepping, AIChE J. 56 (2010) 1739–1747.
[74] B. Espinasse, P. Bacchin, P. Aimar, On an experimental method to measure critical flux in ultrafiltration, Desalination 146 (2002) 91–96.
[75] P. Bacchin, P. Aimar, R.W. Field, Critical and sustainable fluxes: theory, experiments and applications, J. Membr. Sci. 281 (2006) 42–69.
[76] D. Jiao, M.M. Sharma, Mechanism of cake buildup in crossflow filtration of colloidal suspensions, J. Colloid Interface Sci. 162 (1994) 454–462.
[77] Z. He, D.J. Miller, S. Kasemset, D.R. Paul, B.D. Freeman, The effect of permeate flux on membrane fouling during microfiltration of oily water, J. Membr. Sci. 525 (2017) 25–34.
[78] R. Ghosh, Study of membrane fouling by BSA using pulsed injection technique, J. Membr. Sci. 195 (2002) 115–123.
[79] D.M. Kanani, R. Ghosh, A constant flux based mathematical model for predicting permeate flux decline in constant pressure protein ultrafiltration, J. Membr. Sci. 290 (2007) 207–215.